Realizing Biorefineries by Expanding the Sugars Platform: Monosaccharide Separation

Paul Albertus
Department of Energy – Energy Research Undergraduate Laboratory Fellowship Program
University of Michigan, Ann Arbor
National Renewable Energy Laboratory
Golden, Colorado

August 10, 2001

Prepared in partial fulfillment of the requirements of the Department of Energy ERULF Program under the direction of Keith Neeves in the Biotechnology Division for Fuels and Chemicals at the National Renewable Energy Laboratory.

Participant:

_____

Signature

Research Advisor:

_____

Signature

ABSTRACT **3**

INTRODUCTION **4**

PROCESS DIAGRAM 6
SEPARATION MECHANISM 7

MATERIALS AND METHODS **7**

EQUIPMENT 7
PULSE TEST PREPARATION 9
CONDUCTING A PULSE TEST 9

RESULTS **10**

DISCUSSION AND CONCLUSIONS **11**

ACKNOWLEDGEMENTS **14**

REFERENCES **15**

CHARTS AND FIGURES **16**

FIGURE 1. SIMPLIFIED BLOCK FLOW DIAGRAM FOR BIOMASS-TO-ETHANOL PROCESS 16
TABLE I. APPROXIMATE COMPOSITION OF DILUTE-ACID 16
HEMICELLULOSIC HYDROLYSATE 16
FIGURE 2. SIZE EXCLUSION CHROMATOGRAPHY 17
FIGURE 3. STRUCTURES OF THE MONOSACCHARIDES PRESENT IN HEMICELLULOSE. 17
FIGURE 4. EXPERIMENTAL APPARATUS USED TO CONDUCT EACH PULSE TEST 18
FIGURE 5. PERISTALTIC PUMP CURVE 18
FIGURE 6. PURE COMPONENT ISOTHERMS AT VARIOUS CONCENTRATION FOR XYLOSE. 19
FIGURE 7. ISOTHERMS FOR ALL FIVE SUGARS INJECTED IN A SINGLE PULSE 19
TABLE II. PURE COMPONENT ELUTION TIMES AT VARIOUS CONCENTRATIONS 20
TABLE III. COMPETITIVE ISOTHERM DATA. 20
TABLE IV. VARYING FLOW RATE AND COLUMN LENGTH 20
FIGURE 8. EXPERIMENTAL DATA AND MODEL CURVE FOR GLUCOSE PULSE AT 22.5 G/L. 21

Abstract

Realizing Biorefineries by Expanding the Sugar Platform: Monosaccharide Separation. Paul Albertus (University of Michigan, Ann Arbor, MI, 48109) Keith Neeves (National Renewable Energy Laboratory, Golden, CO 80401).

The development of a biorefinery – a plant fed only by biomass and capable of producing multiple products, from fuels to plastics to pharmaceuticals – represents an important step toward the transformation to a sustainable society. The monosaccharides of biomass – glucose, xylose, mannose, galactose, and arabinose - may serve as the basis for a renewable chemicals industry. In order to take advantage of each monosaccharide's unique structure they must be separated from each other and the other components of biomass. Simulated moving bed (SMB) chromatography is one method for industrial scale sugar separations. Its complexity requires that a computer model be used to predict flow rates and switching times. Therefore, batch chromatography was used to determine the values of the parameters needed to construct a computer model of a SMB system. Pure component isotherms for each of the five monosaccharides at various concentrations, and competitive isotherms, in which multiple monosaccharides were included in a single pulse, were gathered. Flow rate and column length was varied to determine their effect on elution profiles. From these isotherms, it was clear that for monosaccharide concentrations similar to that from a slipsteam of hydrolysate from a bioethanol process, elution time is independent of monosaccharide concentration and the presence of multiple monosaccharides. Increasing residence time only modestly improved the separation. The computer model generates theoretical elution profiles that can be matched to the experimental ones by varying flow parameters. The correct parameters will be used by the model to aid in a full-scale experimental verification of the separation.

Research Category (Please Circle)
ERULF: Physics Chemistry Biology Engineering Computer Science Other_____

School Author Attends: University of Michigan, Ann Arbor
DOE National Laboratory Attended: National Renewable Energy Laboratory
Mentor's Name: Keith Neeves
Phone: (303) 384-6847
Email Address: keith_neeves@nrel.gov

Presenter's Name: Paul Albertus
Mailing Address: 2540 Meadowview Ct.
City/State/Zip: Rochester Hills, MI 48306
Phone: (248) 651-5224
Email Address: paul_albertus@nrel.gov

Introduction

Among the challenges of the 21st century, one of the most pressing will be the need to develop a sustainable supply of material resources and energy that do not cause long-term environmental change. Among the developing areas of technical expertise, perhaps the most significant will be that derived from an increasing understanding of biological systems (Lynd et al., 1999). Thus, the application of biotechnology to further sustainability goals responds to this principal challenge with a rapidly developing ability, perhaps providing a solution of one of the most difficult problems faced today.

One developing area of research uses biotechnology to aid in the conversion from a petroleum-based economy to one that relies on alternative and renewable sources of carbon for fuels, chemicals, and energy. Biomass—nonfood cellulosic plant material—is the primary candidate for a variety of environmental and economic reasons (Lynd et al., 1999). Among the most notable are its rich chemical diversity, large and renewable supply, and low cost. However, biomass processing technologies are still in a relatively nascent stage, except for the one that produces ethanol (Lynd et al., 1991). Ethanol often receives the most attention because of its use as an octane enhancer in petroleum based fuels. This will be especially important considering the gap in octane due to the MTBE phase-out across the United States. However, a multitude of valuable products besides ethanol can be produced from biomass. For example, the sugars of lignocellulosic biomass may serve as the feedstock of an economically viable renewable chemicals industry. Ultimately, a "biorefinery" will exploit multiple market opportunities by supplying a wide range of products from plastics to fuels to pharmaceuticals from a single feedstock, just as a petroleum refinery does today.

Toward this end, previous work has focused on the separation of the sugars of biomass – glucose, xylose, mannose, galactose, and arabinose - from toxic components (e.g. sulfuric and acetic acid) formed during an initial acid hydrolysis stage in the biomass-to-ethanol conversion process (Wooley, 1998). Once a sugar stream has been isolated, the unique chemical properties of each individual monosaccharides can be capitalized on. Xylose, especially, has currently untapped market potential (Neeves et. al., 2001). Production of several low volume, high value monosaccharide products, in addition to the high volume, low value ethanol, would aid in the creation of a biorefinery because of the economic benefits of co-production.

The purpose of this work, therefore, was to expand our ability to carry out an effective separation of the monosaccharides of biomass, when supplied as a stream from a biomass-to-ethanol process. Such a separation would be carried out on an industrial scale using simulated moving-bed (SMB) chromatography, which links a series of individual columns and uses a central valve to vary input and output positions (Nicoud et al., 2000). The operation of an SMB system requires that system dimensions, such as bed length and diameter, resin characteristics, such as internal and external porosity, and flow characteristics, such as axial dispersion, film coefficient, and retention factor, be known (see Ma et al., 1997 for notation explanations and modeling theory). Of these, the flow characteristics must be extracted from experimentally generated elution profiles. Once they are known a computer model can be constructed that will compute flow rates and switching times, making start-up of an actual SMB system much easier. Specifically, the pure component isotherm for each monosaccharide, competitive isotherms with multiple monosaccharides, and the effects of flow rate or column length on dispersion are needed

for the successful completion of the computer model. This model can also be used to determine the technical and economic viability of the attempted separation.

Process Diagram

The sugar separation stage developed in this work will ultimately be implemented as one stage in an integrated biomass-to-ethanol process. Ideally, product production levels could be varied according to market conditions in order to maximize economic return. Figure 1 is a block flow diagram of the process. Biomass feedstock is first prepared for processing by washing (to remove dirt or other soluble impurities) and sifting (to insure homogenous particle size). It is then fed into a reactor and mixed with dilute sulfuric acid. This breaks down the polysaccharide hemicellulose into its five component monosaccharides and acetic acid. It also breaks down some of the entering cellulose (a biopolymer of glucose). It is from the output of this stage that a slipstream of hydrolyzate could be withdrawn and, following their separation from the two acids, the individual monosaccharides isolated and purified. Typical concentrations of the components of the output of the acid hydrolysis stage can be found in Table I. The remaining hydrolyzate continues to the fermentation stage where it undergoes Simultaneous Saccharification and Co-Fermentation (SSCF), in which the remaining cellulose is enzymatically hydrolyzed while fermentation of all the monosaccharides simultaneously occurs. The fermentation sludge is then purified by distillation and a molecular sieve to reach an anhydrous ethanol product. Eventually, multiple fermentation trains could be used in a biorefinery for multiple product production. Solid waste from the process is burned to meet heat and energy requirements.

Separation Mechanism

Sugar separations were carried out using batch column chromatography. Dowex Monosphere 99CA/320 Separation Resin was used, following the literature for the separation of glucose, xylose, and arabinose, as well as the recommendation for its use by an employee of Dow Chemical (Balannec et al., 1993, Pynonnen, 2001). Dow Chemical designed this resin for the separation of glucose and fructose; it utilizes a ligand exchange mechanism to slow the elution of fructose. None of the sugars in this study have a ligand equivalent to that of fructose, so theoretically the separation relies instead on a size exclusion mechnanism in which larger molecules elute faster because they are too large to fit inside the small openings in the resin particles. Figure 2 is a visual representation of the separation mechanism. In it, the ovals correspond to smaller molecules, which are more likely to become entangled in the resin and therefore elute through the column more slowly. The pentagons correspond to molecules that are too large to enter the resin particle mesh, and therefore pass through it more quickly. The separation of the monosaccharides of biomass is difficult because of their chemical and size similarities. This is readily apparent from their structures, given in Figure 3, as well as their molecular weights (150 AU for arabinose and xylose, 180 AU for glucose, mannose, galactose).

Materials and Methods

Equipment

Figure 4 is a diagram of the experimental apparatus. The glass, jacketed column (Ace Glass, part 5821-112) used in the experiments had a length of 120 cm and a internal diameter of 2.61 cm. The resin used was Dowex Monosphere 99CA/320 Separation

Resin (obtained from Supelco, part 13721), charged with calcium ions and with an average resin particle diameter of 320 μm. Bulk porosity was measured by heating the column to 65° C, drawing the eluant to the surface of the resin, and then draining a single bed volume into a beaker. Its volume was measured and bulk porosity calculated as (collected eluant volume)/(total bed volume). A polyethylene float with a diameter of 2.5 cm was placed on top of the column to prevent the falling eluant from disturbing the surface of the resin. A 20 cc syringe was used to inject the pulse. The separation column was connected to a second, smaller column (Ace Glass, part 5821-24) that served as a preheater for the eluant. It had an internal diameter of 2.5 cm and a length of 30 cm. A hot recirculating water bath kept both columns at a constant temperature of 65° C. To transport fluid through the system, two peristaltic pumps were used (Watson-Marlow, model 101U). One directed eluant into the pre-heater, and the second drew fluid out of the bottom of the column loaded with resin. The flow rate of this second pump was carefully measured, as it controlled the rate at which fluid was drawn through the bed. Figure 5 contains the pump curve for this second pump. Samples were collected using a fraction collector (Gilson, model FC-80K). A densiometer connected to the output from the separation column provided a rough estimate of when the pulse had traveled through the column (Paar, mPDS 2000). The concentration of the collected samples was determined by HPLC using a Hewlett Packard 1090 with an RI detector, and either a Biorad Aminex HPX-87H column running 0.01 N sulfuric acid as a mobile phase, or a Biorad Aminex HPX-87P column using deionized (DI) water. The HPX-87H column had a hydrogen resin and was capable of separating and detecting glucose, xylose, and

arabinose. When mannose or galactose was present in the sample, the HPX-87P column, which had a lead resin, was used.

Pulse Test Preparation

After obtaining and setting up the necessary equipment, we mixed the resin into a beaker with DI water to form a slurry, which was poured into the top of the column. The bed depth was adjusted to the proper height for the experiment being run (either 97.5 cm or 215.9 cm). DI water was backwashed through the column to insure that there was no air in the resin. This was critically important, as any air in the bed could have disturbed the elution of the pulse. For this reason the DI water that served as the eluant was deaerated.

Conducting a Pulse Test

After the entire system reached a state of equilibrium (a constant 65°C), the eluant was drawn down to the top of the resin, and any remaining eluant in the tubing between the syringe and the top of the column was emptied to prevent it from mixing with the pulse. The eluant feed was subsequently shut off and the pulse injected into the column over approximately 30 seconds. Again, any fluid from the pulse trapped in the tubing between the syringe and the top of the column was emptied. Timing began when the pump withdrawing liquid from the column was started. After the pulse was completely drawn into the resin, the eluant feed was restarted so that the level of the fluid in the column was never drawn beneath the surface of the resin. The eluant feed rate was adjusted so that while the pulse traveled through the column there was a constant depth of eluant above the top of the resin. The densiometer was used to track the flow of the pulse through the column so that fraction collection could start and end at an appropriate time

(starting a few minutes before the leading edge of the pulse was expected, ending a few minutes after the trailing edge passed through).

Results

When a bed with a volume of 521 ml was drained to determine bulk porosity, 160ml were collected. The value for the bulk porosity was therefore .307. Using a flow rate of 9.4 ml/min the leading edge of the pulse, assuming no dispersion, should have appeared at around 17 min. But even the leading edge of the pulses with high monosaccharide concentrations did not begin to appear until after 24 min.

A primary objective of this project was to characterize the elution curve of each monosaccharide as it traveled through the column. Figure 6 shows a representative pure component isotherms (xylose). If analystical error from HPLC analysis, which varied as determined by comparison with a calibration verefication standard, exceeded 5% the samples were analyzed again. The error bars on Figures 6, 7, and 8 correspond to this maximum possible error. However, error was typically under 2.5%. As Figure 6 demonstrates, the elution profile is independent of the concentration of the pulse; the maximum concentration is reached at the same time regardless of concentration. This was also true for the isotherms of glucose, galactose, arabinose, and mannose. Table II contains the elution time vs. concentration for each of the monosaccharides when injected as a pure component. Small variations in elution times are due to experimental error and not independently controlled variables, such as pulse concentration. For example, mean peak xylose elution time was 33.09 +/- 0.079748 min within a 95% confidence interval and showed no trend to change with concentration.

Competitive isotherms, in which two or more different sugars were combined in a single pulse, were also gathered. Elution times of the pure components in the competitive isotherms were not affected by the presence of a different sugar or its concentration. Table III, a matrix of the competive isotherms and the elution times for each component, clearly shows this.

Figure 7 presents a plot of the elution profile of a pulse that contained all 5 monosaccharides, in concentrations approximately equal to that found in the hydrolysate slipstream (see Table I). Because the sugars elute at approximately the same time and dispersion results in pulse overlap, efforts to improve the separation were made by varying residence time by either changing the flow rate or the column length. To measure the effects of these changes, we injected a pulse of glucose at 10g/l and xylose at 50 g/l and recorded the elution times. The results of these experiments can be found in Table IV.

Discussion and Conclusions

The fact that the monosaccharides elute through the column significantly slower (24 min, at the earliest) than the eluant (17 min) verifies that the resin is indeed interacting with the molecules through dispersion in and out of the resin pores or by diffusion through the gel-like medium of the resin bed.

The fact that elution time for each single component is independent of concentration and the presence of other monosaccharides is supported by literature sources that estimate saturation concentration for the Dowex 99 resin to be in the range of 350 to 400 mg/g (Balannec et al., 1993). Therefore, for sugar concentrations up to 100g/L the isotherms should be linear. The highest sugar concentration used in a pulse

test in this set of experiments was 73.5 g/L (in the pulse containing all five sugars at the concentrations shown in Figure 7).

Figure 7 illustrates the principal difficulty with the separation of the monosaccharides from biomass; their structural similarity results in similar elution times, and axial dispersion results in significant overlap. The attempts to improve the separation by decreasing the flow rate or increasing the bed length did increase the time interval between the maximum concentration of each component, as shown in Table IV. However, pulse dispersion also increased, preventing the possiblity of a significantly better separation. For example, the best separation of glucose and xylose, based on purity and yield, was achieved with the bed length at 217.2 cm and a flow rate of 9.4 ml/min. Peak separation was 5.5 minutes, as opposed to 2.3 minutes for a bed length of 97.5 cm and the same flow rate. However, for the longer column the glucose concentration was above .2 g/l for 18 minutes, and the xylose concentration for 24 min. For the shorter column those numbers were 13 min and 17 min, respectively. Thus, increasing residence tended to move the peaks apart but also broadened them.

So what does this mean for the possibility and efficacy of the desired separation? Can glucose and xylose (and perhaps the other monosaccharides) be separated with a yield and purity high enough to ensure economic viability and thereby further the development of a biorefinery? The possiblity of using a SMB system to purify the sugar from the acetic acid and sulfuric acid in the output of the acid hydrolysis stage has been demonstrated (Wooley et al., 1999). Further, the separation of glucose, xylose, and arabinose with high purities and yields has been demonstrated using both batch chromatography and an SMB system (Balannec et al., 1993). However, as a testament to

the difficulty of that separation, in some batch experiments the authors used bed lengths in excess of 20 m and flow rates under 5 ml/min corresponding to residence times in excess of 40 hours. For the operation of an SMB system to achieve this separation the authors forcefully stress that a computer model is absolutely necessary in order for the operation of a commercial system, because with the specified flow rates and column lengths steady state operation was reached very slowly, and it is only at steady state operation that system performance can be evaluated. It was due to this necessity that the batch experiments presented here were carried out, and the necessary information gathered for the completion of a computer model.

The model is based on a pair of coupled partial differential equations (PDE) that describe the motion of the pulse through the chromatography resin. These equations link product purity and recovery to properties of the SMB system such as zone length, bed movement velocity, flow rates, column capacity factors, and mass transfer coefficients (Ma et. al., 1997). Simulations use a finite difference model that divides the column into a large number of short sections, over which flow is modeled. The partial differential equations are then systematically applied to each interval to predict flow. That prediction of pulse behavior is made by a numerical integrator such as the forward Euler, backward Euler, or a Runga-Kutta method. Thus, the simulation yields a concentration versus time curve that can be compared with the ones gathered experimentally. The unknown constants in the partial differential equations (axial dispersion, film coefficient, and retention factor) are varied until the simulated curve matches the experimental one. Once this curve fit is made the unknown constants have been determined and the fundamental information needed to construct a model of an SMB system has been obtained.

Figure 8 shows an example of a pulse elution curve generated by the model superimposed on experimental data. The data is for a pulse of glucose with a concentration of 22.5 g/l. The Runga-Kutta method was used for integration. K_f, the film coefficient, was varied to match the dispersion of the pulse. δ, the retention factor, controlled the time of peak concentration. As that figure shows, when K_f is set to 1.35, and δ is set to .366, the theoretical curve passes through nearly all the experimental data. Ultimately, these parameter values will be used for not only the simulation of a batch chromatography experiment, but also a SMB system.

This model will be a powerful tool that will both aid in the startup of the onsite SMB system by providing estimates for initial operating parameters and furnish results that will determing the economic feasibility of the separation and purification methods. It should provide valuable guidance to those seeking to make biorefineries a reality.

Acknowledgements

First, I would like to thank my mentor, Keith Neeves, for organizing and guiding my research. Thanks also go to the DDRD biorefinery team, especially John Jechura. I would also like to acknowledge Ray Ruiz and David Templeton for their indefatigable help in debugging the HPLC systems. Linda Lung and Robi Robichaud did an excellent job organizing and running the ERULF program, of which I was a part. And finally, thanks to the Department of Energy for funding the research, and the National Renewable Energy Lab for hosting me and for its foresight in recognizing the inevitable need for a sustainable America and World.

References

Balannec, B.; Hotier, G. (1993). "From Batch to Countercurrent Chromatography," Chapter 14. Ganetsos, G.; Barker, P. E. ed. Preparative and Production Scale Chromatography. Marcel Dekker, Inc., New York, pp. 301-357.

Lynd, L. R.; Cushman, J. H.; Nichols, R. J.; Wyman, C. E. (1991). "Fuel Ethanol from Cellulosic Biomass." Science. 251(4999): pp. 1318-1323.

Lynd, L. R., Wyman, C. E., Gerngross, T. U. (1999). "Biocommodity Engineering." Biotechnol. Prog., 15 (5): pp. 777-793.

Ma, Z.; Wang, N.-H.L. (1997). "Standing Wave Analysis of SMB Chromatography: Linear Systems," AIChE Journal, 43(10): pp. 2488-2508.

Neeves, K. (2001). NREL Technical Memorandum, http://www.afdc.doe.gov/bcfcdoc/5597.doc.

Nicoud, R. M.; Majors, R. E. (2000). "Simulated Moving Bed Chromatography for Preparative Separations." LCGC., 18(7): pp. 680-687.

Pynonnen, B. (2001). Personal Communication. Dow Chemical Company.

Wooley, R.; Ma, Z.; Wang, N.-H. L. (1998) "A Nine-Zone Simulating Moving Bed for the Recovery of Glucose and Xylose from Biomass Hydrolyzate." Ind. Eng. Chem. Res., 37: pp. 3699-3709.

Charts and Figures

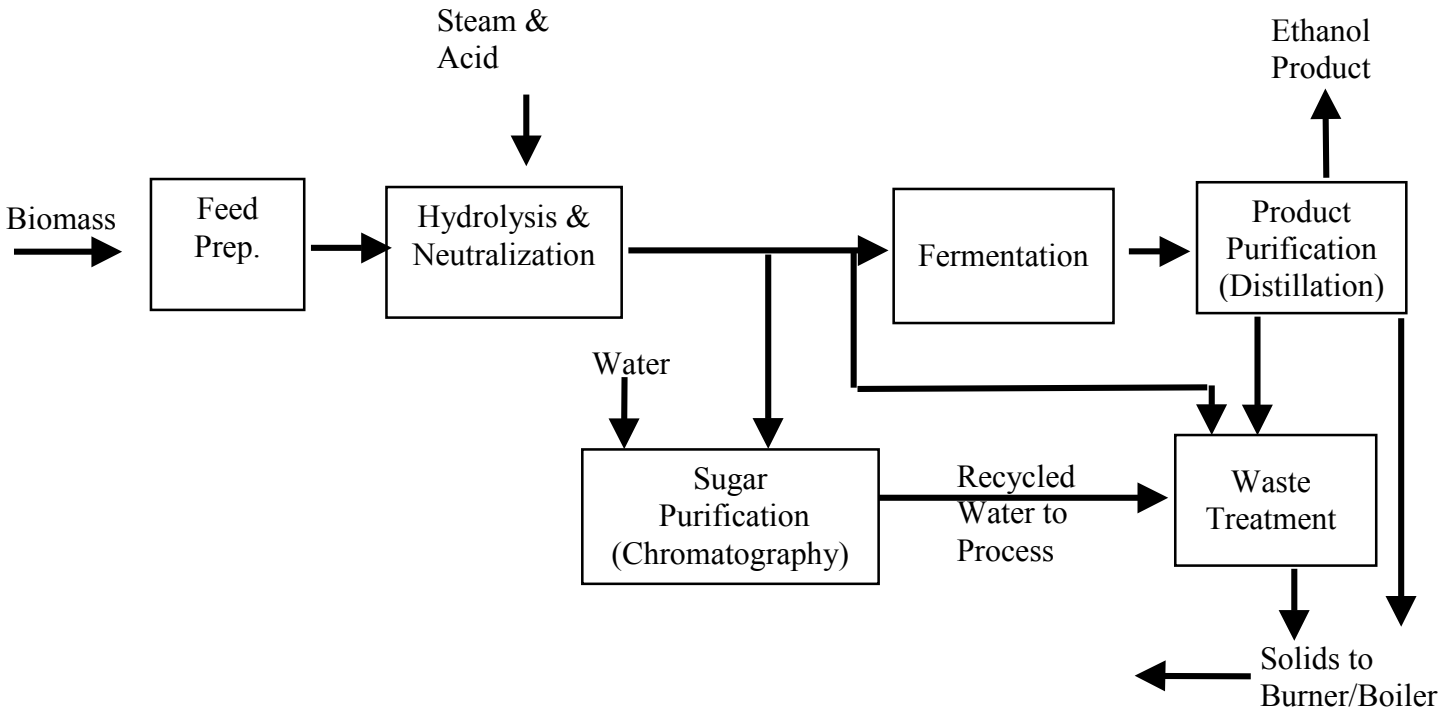

Figure 1. Simplified block flow diagram for biomass-to-ethanol process

Table I. Approximate composition of dilute-acid hemicellulosic hydrolysate

Component	Concentration (g/L)
Glucose	7.9
Xylose	52.1
Arabinose	6.7
Galactose	3.6
Mannose	0.5
Oligomers	7.7
Proteins	14.5
Furfural	4.6
Hydroxymethyl Furfural	0.4
Acetic Acid	0.7

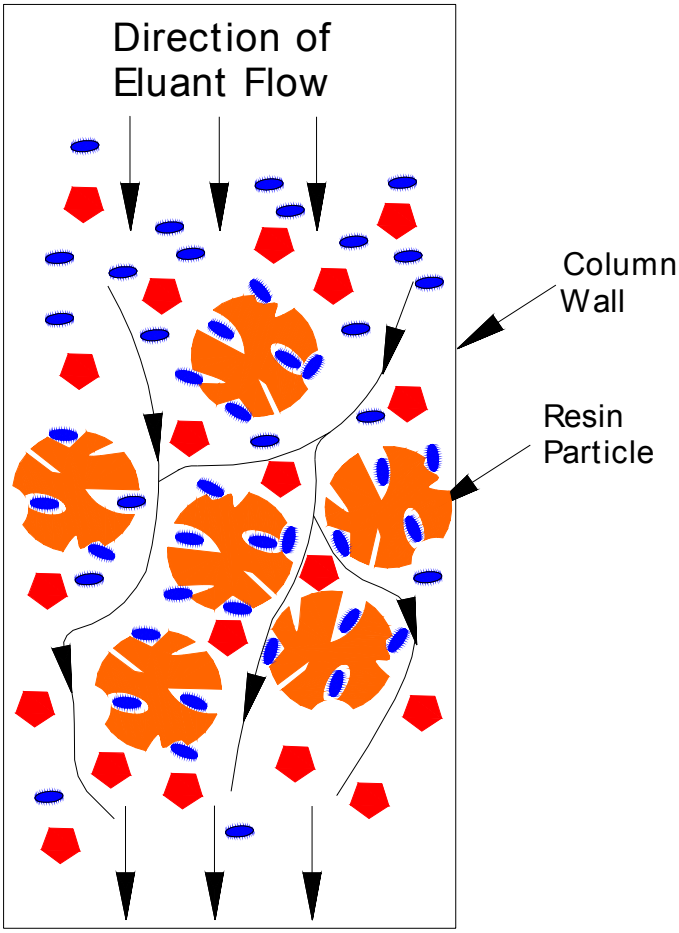

Figure 2. Size exclusion chromatography
Represent 'large' molecules
Represent 'small' molecules
Note: The resin diameter is not to the scale of the column width

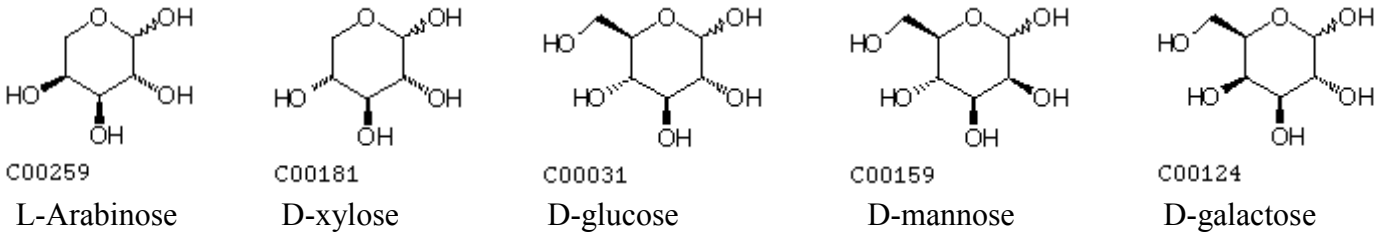

Figure 3. Structures of the monosaccharides present in hemicellulose.

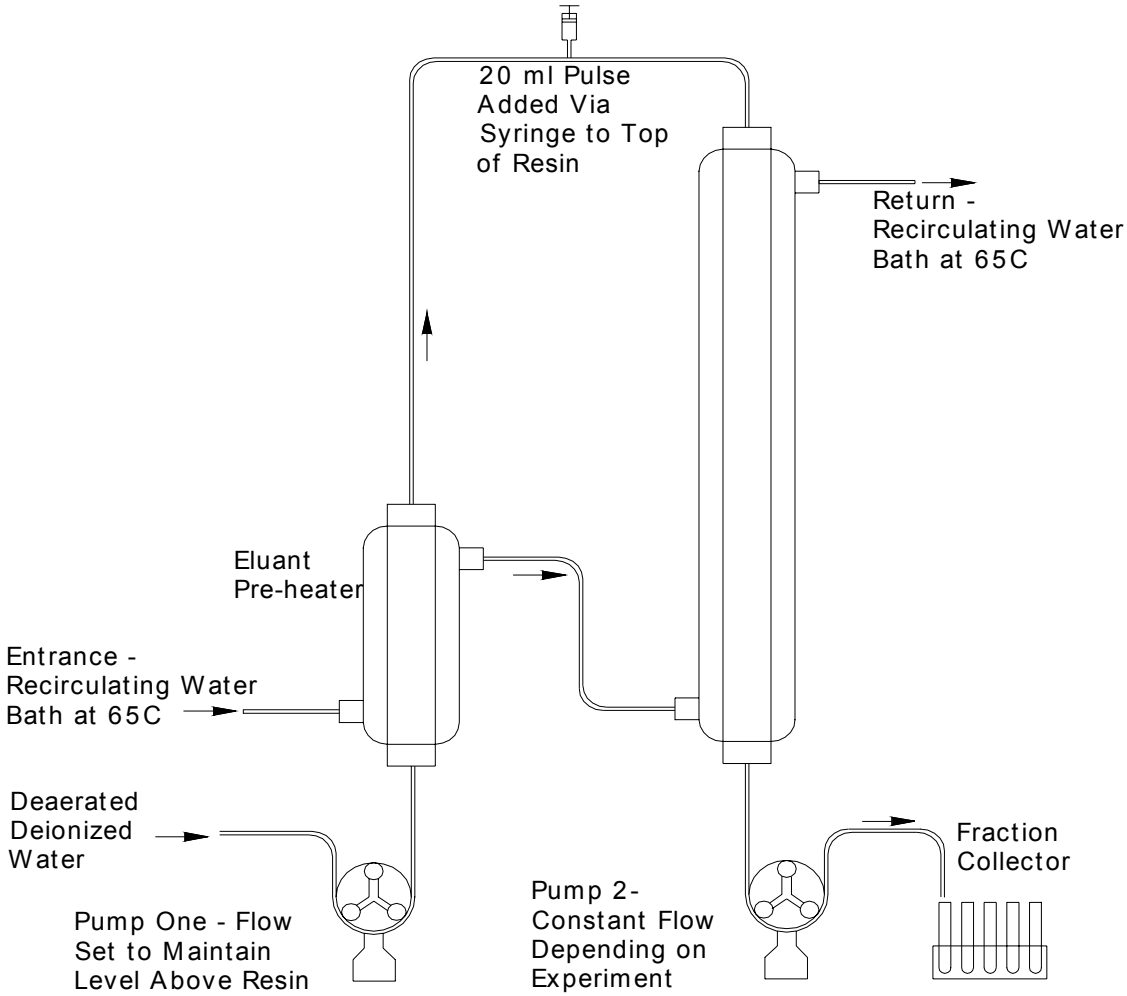

Figure 4. Experimental apparatus used to conduct each pulse test

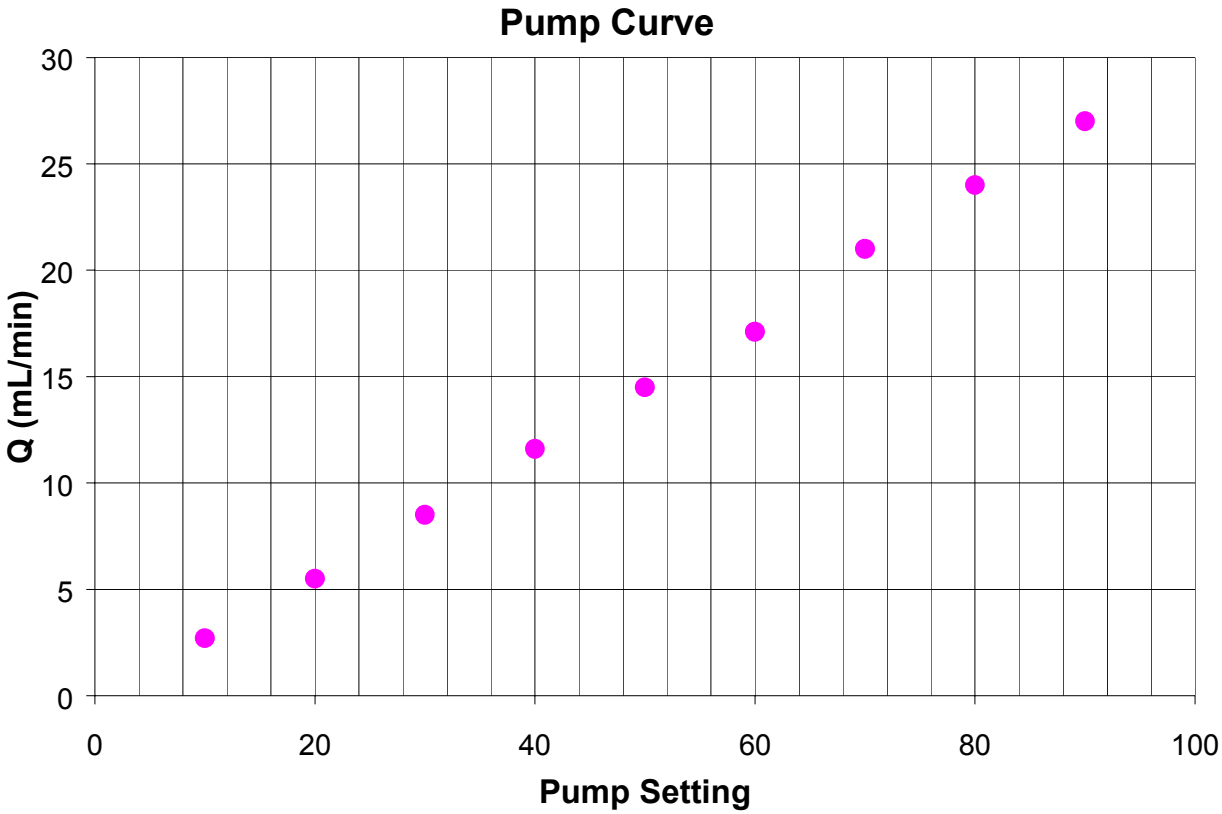

Figure 5. Peristaltic pump curve

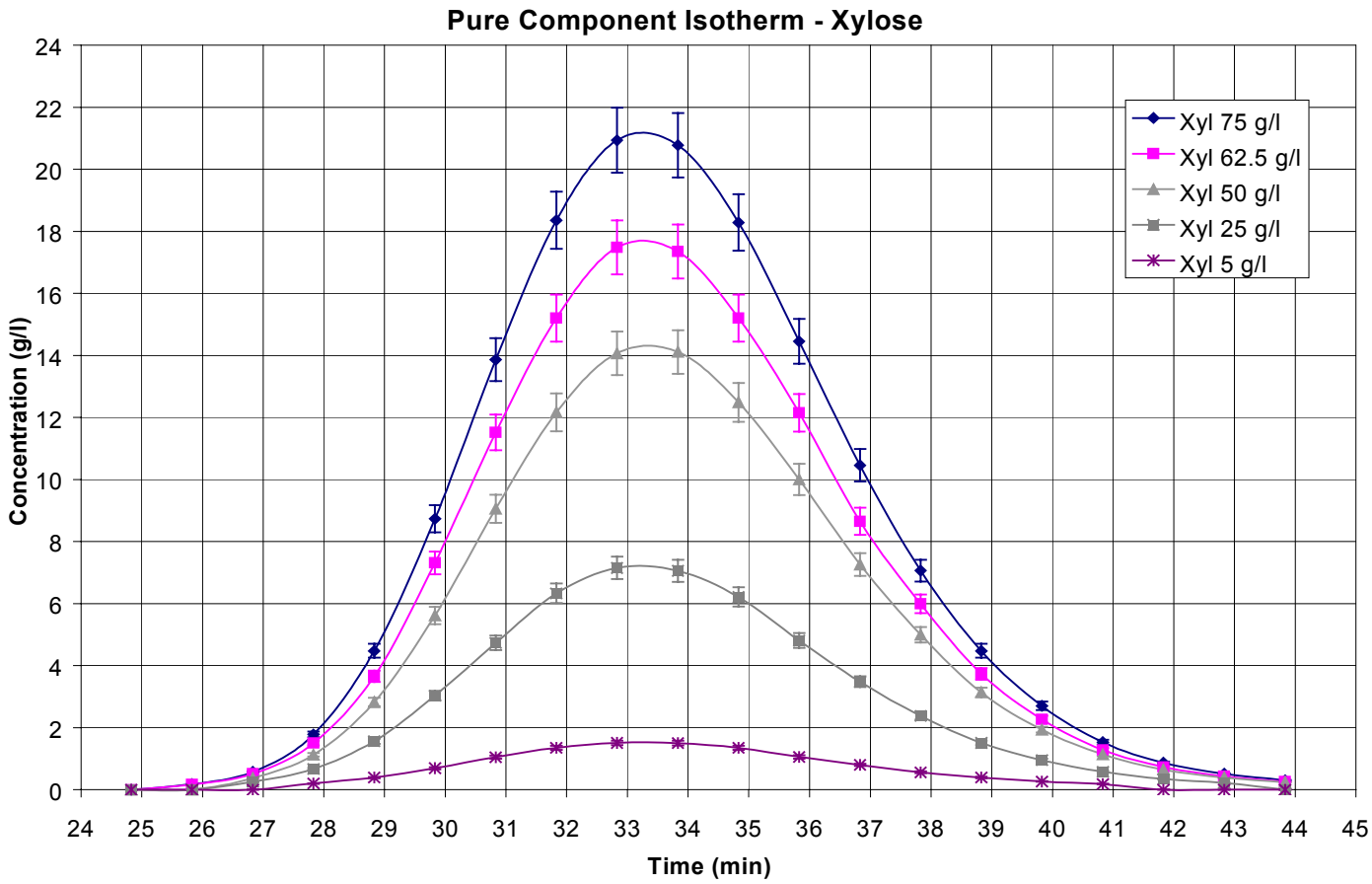

Figure 6. Pure component isotherms at various concentration for xylose. Note that elution time is independent of pulse concentration.

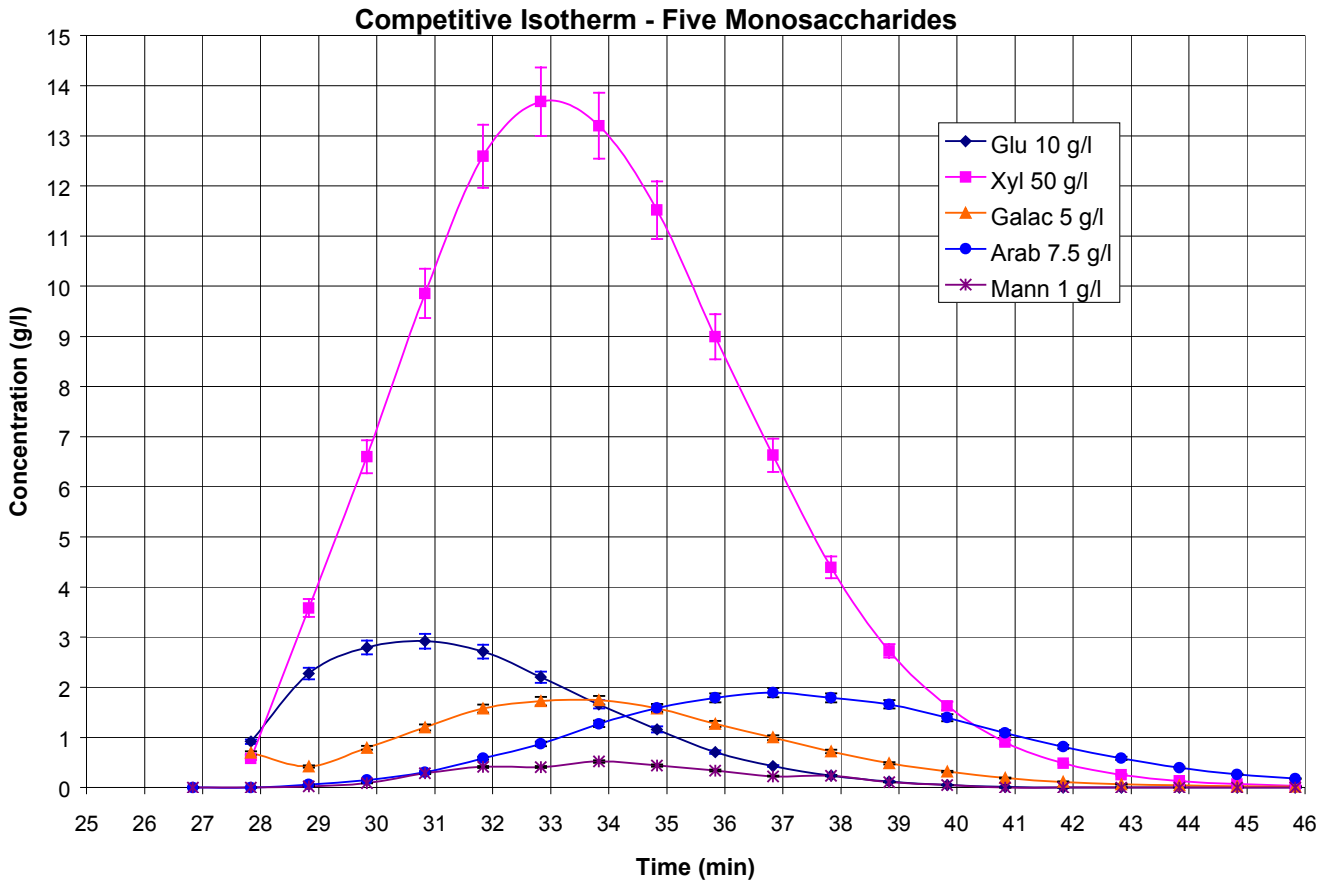

Figure 7. Isotherms for all five sugars injected in a single pulse

Table II. Pure component elution times at various concentrations

Compound	Concentration (g/l)	Elution Time (min)
Glucose	22.5	31.0
	18.75	30.8
	15	30.5
	7.5	30.7
	1.5	30.8
Xylose	75	33.2
	62.5	33.2
	50	33.2
	25	33.1
	5	33.2
Mannose	10	34
	5	32.5
	1	34
Arabinose	15	37
	7.5	37
	1	36.5
Galactose	10	33.5
	5	33
	1	32.5

Table III. Competitive isotherm data

Concentration (g/l)					Elution Time (min)				
Glu	Xyl	Arab	Mann	Galac	Glu	Xyl	Arab	Mann	Galac
25	5	0	0	0	30.8	33.0			
10	50	0	0	0	31	33.2			
1.5	75	0	0	0	30.8	32.9			
10	50	7.5	1	5	30.7	32.9	37	33.8	33.5
10	10	10	10	10	30.9	33.3	37.5	33.9	33.6

Table IV. Varying flow rate and column length

Flow Rate (ml/min)	Column Length (cm)	Elution Time (min)	
		Glucose	Xylose
20.0 ml/min	97.5	14.6	16.0
9.4 ml/min	97.5	31.0	33.2
4.9 ml/min	97.5	62.5	67.0
1.1 ml/min	97.5	260	270
9.4ml/min	215.9	72	77.5

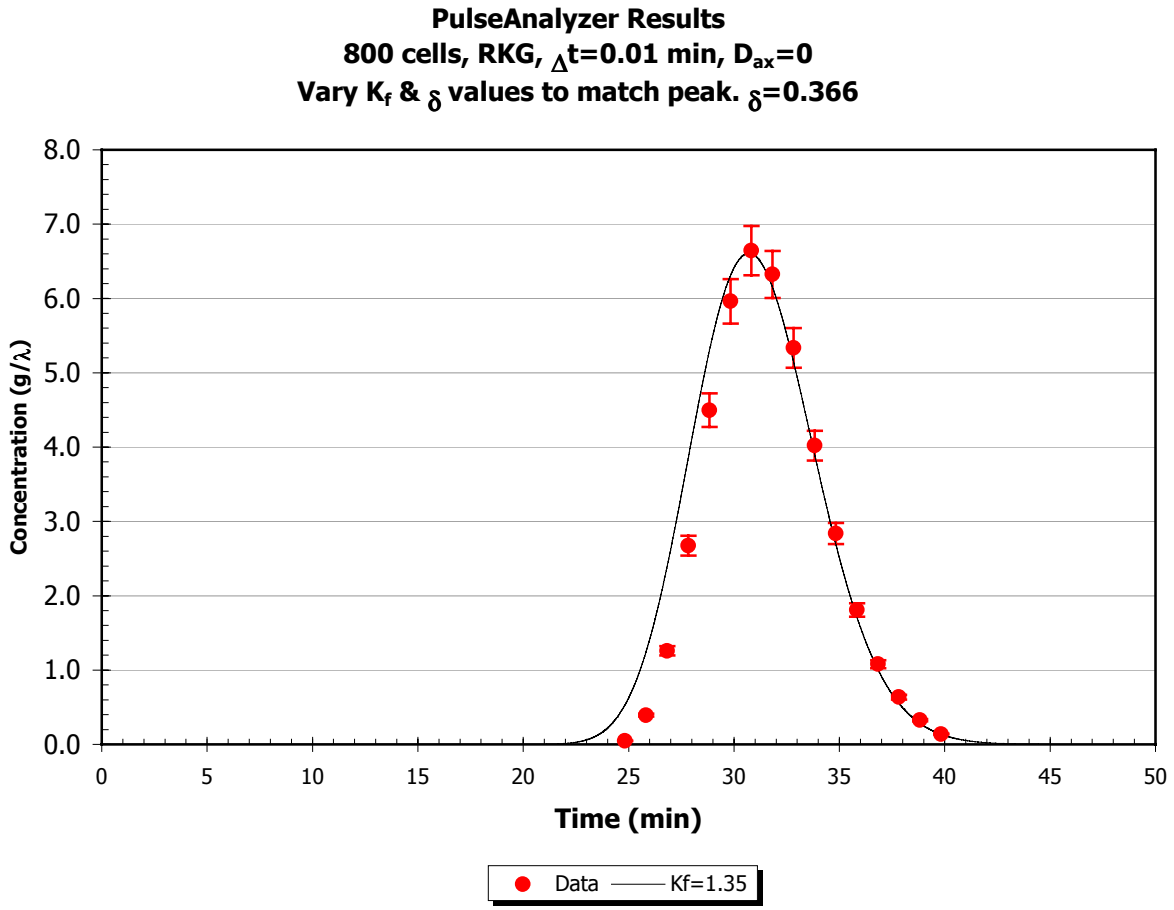

Figure 8. Experimental data and model curve for glucose pulse at 22.5 g/l.